802 *Biochemistry* **2010,** *49,* 802–809
DOI: 10.1021/bi9019127

BIOCHEMISTRY
including biophysical chemistry & molecular biology
Article

Adventitious Arsenate Reductase Activity of the Catalytic Domain of the Human Cdc25B and Cdc25C Phosphatases[†]

Hiranmoy Bhattacharjee,*[,‡] Ju Sheng,[‖] A. Abdul Ajees,[‡] Rita Mukhopadhyay,[§] and Barry P. Rosen[‡]

[‡]*Department of Cellular Biology and Pharmacology, and* [§]*Department of Molecular Microbiology and Infectious Diseases, Florida International University, Herbert Wertheim College of Medicine, Miami, Florida 33199, and* [‖]*Henry Ford Hospital, Detroit, Michigan 48202*

Received November 6, 2009; Revised Manuscript Received December 18, 2009

ABSTRACT: A number of eukaryotic enzymes that function as arsenate reductases are homologues of the catalytic domain of the human Cdc25 phosphatase. For example, the *Leishmania major* enzyme LmACR2 is both a phosphatase and an arsenate reductase, and its structure bears similarity to the structure of the catalytic domain of human Cdc25 phosphatase. These reductases contain an active site C-X_5-R signature motif, where C is the catalytic cysteine, the five X residues form a phosphate binding loop, and R is a highly conserved arginine, which is also present in human Cdc25 phosphatases. We therefore investigated the possibility that the three human Cdc25 isoforms might have adventitious arsenate reductase activity. The sequences for the catalytic domains of Cdc25A, -B, and -C were cloned individually into a prokaryotic expression vector, and their gene products were purified from a bacterial host using nickel affinity chromatography. While each of the three Cdc25 catalytic domains exhibited phosphatase activity, arsenate reductase activity was observed only with Cdc25B and -C. These two enzymes reduced inorganic arsenate but not methylated pentavalent arsenicals. Alteration of either the cysteine and arginine residues of the Cys-X_5-Arg motif led to the loss of both reductase and phosphatase activities. Our observations suggest that Cdc25B and -C may adventitiously reduce arsenate to the more toxic arsenite and may also provide a framework for identifying other human protein tyrosine phosphatases containing the active site Cys-X_5-Arg loop that might moonlight as arsenate reductases.

Arsenic ranks first on the U.S. Department of Health and Human Services Superfund Priority List of Hazardous Substances (http://www.atsdr.cdc.gov/cercla/07list.html). Exposure to inorganic arsenic occurs primarily through geochemical sources, although anthropogenic sources also contribute. Chronic exposure to arsenic primarily from drinking water has been linked to cardiovascular, peripheral vascular, and cerebrovascular disease, diabetes, and cancer (*1*). The two biologically important oxidation states of arsenic in the environment are the pentavalent arsenate [As(V)] and trivalent arsenite [As(III)] forms. As(III) is more toxic than As(V) and is primarily responsible for the biological effects of arsenic.

As our environment is highly oxidizing, arsenicals are frequently present in the pentavalent form. Although As(V) can be reduced to As(III) nonenzymatically, this process is too slow to be physiologically significant, and organisms utilize enzymes to catalyze As(V) reduction (*2*, *3*). Several mammalian enzymes that apparently catalyze arsenate reduction have been reported recently, including purine nucleoside phosphorylase, glyceraldehyde-3-phosphate dehydrogenase, glycogen phosphorylase-a, phosphotransacetylase, and arsenite *S*-adenosylmethyltransferase (*2*, *4*), although it is not clear whether any of these enzymes function physiologically in the reduction of As(V). On the other hand, genuine arsenate reductases that catalyze the two-electron reduction of inorganic As(V) to As(III) have been reported in many prokaryotes and eukaryotes. These enzymes arose independently at least three times by convergent evolution. One family of arsenate reductase that includes *Escherichia coli* plasmid R773 ArsC uses glutaredoxin (Grx)[1] and glutathione (GSH) as reductants (*3*). *E. coli* has three glutaredoxins, Grx1, Grx2, and Grx3, any one of which will serve as the source of reducing potential for arsenate reduction, although Grx2 is preferred (*5*). Homologues of this *arsC* gene have been found in many bacteria, both on plasmids and in chromosomes. A second family of arsenate reductases also widely distributed in bacteria is typified by the *arsC* gene product of *Staphylococcus aureus* plasmid pI258 (*6*). Instead of glutaredoxin, the pI258 enzyme uses thioredoxin as the source of reducing potential (*7*) and has two intramolecular cysteine residues that participate in the catalytic cycle (*8*). Interestingly, pI258 ArsC is related to low-molecular weight protein tyrosine phosphatases (LMW-PTPases) and exhibits low-level phosphatase activity (*9*). Both classes of bacterial arsenate reductase described above are involved in arsenic detoxification by reducing arsenate to arsenite, which is then extruded out of the cells either by an arsenite carrier protein, ArsB, where energy is supplied by the membrane potential of the cell (*10*), or by an arsenite-translocating ATPase complex (*3*).

[†]This study was supported by National Institutes of Health Grants AI58170 and GM55425.

*To whom correspondence should be addressed. Telephone: (305) 348-1489. Fax: (305) 348-0651. E-mail: hbhatta@fiu.edu.

[1]Abbreviations: Cdc25-cd, catalytic domain of human Cdc25; DMAs(V), dimethylarsinic acid; GLRX, human glutaredoxin; Grx, glutaredoxin; Grx1p, yeast glutaredoxin; GSH, glutathione; GSR, human glutathione reductase; IPTG, isopropyl β-D-thiogalactoside; MAs(V), monomethylarsonic acid; pNPP, *p*-nitrophenyl phosphate; SDS−PAGE, sodium dodecyl sulfate−polyacrylamide gel electrophoresis.

 Published on Web 12/21/2009 © 2009 American Chemical Society

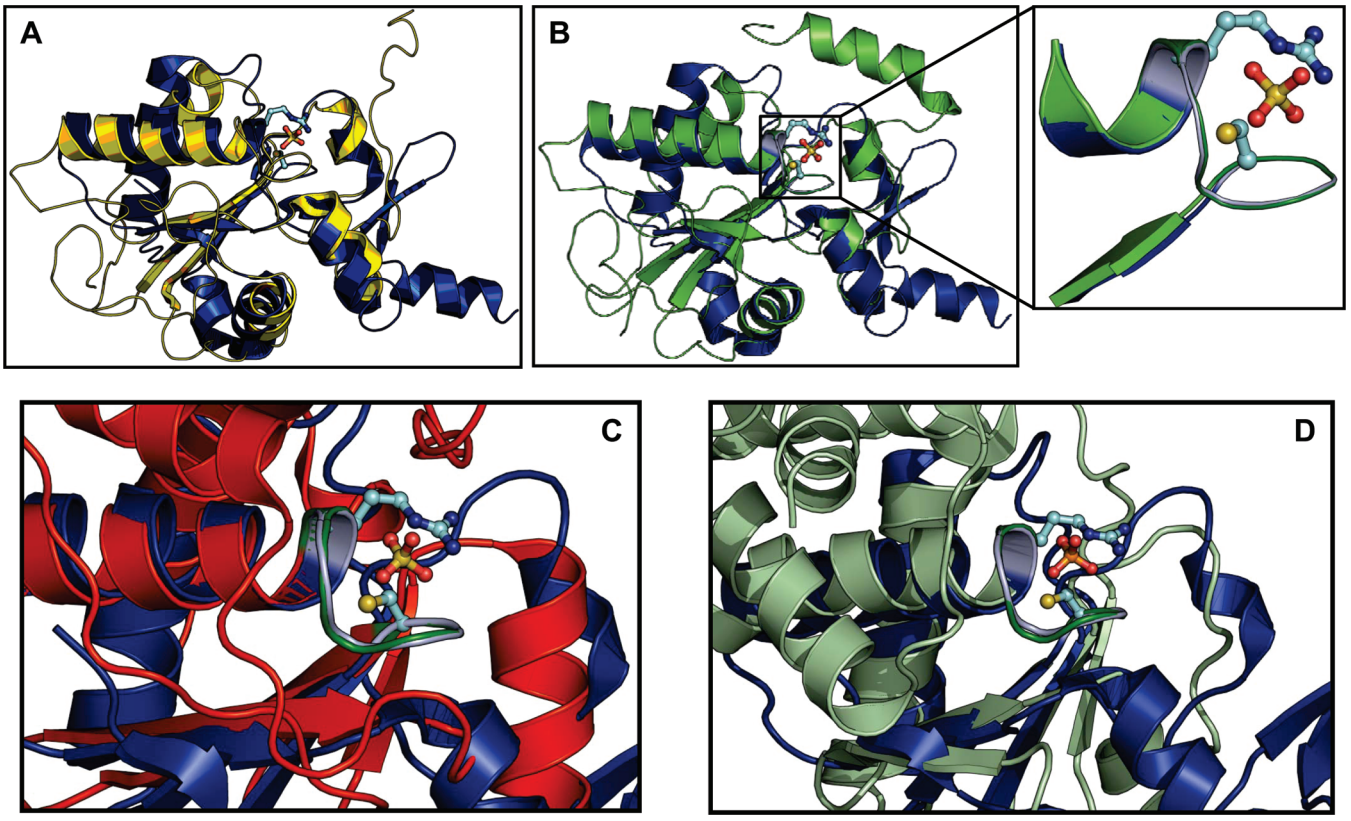

FIGURE 1: Comparison of the active site regions of LmACR2, Cdc25A-cd, Cdc25B-cd, HPTP-B, and DUSP14. Structure of LmACR2 (blue) (PDB entry 2J6P) superimposed on the structure of (A) Cdc25A-cd (golden yellow) (PDB entry 1C25) or (B) Cdc25B-cd (green) (PDB entry 1QB0). The inset shows the C-X_5-R active site loop region for LmACR2 colored light blue and that of Cdc25B-cd colored dark green. The conserved cysteine and arginine residues are shown as ball-and-stick models with the carbon, nitrogen, and sulfur atoms colored cyan, blue, and yellow, respectively. Structure of LmACR2 (blue) (PDB entry 2J6P) superimposed on the structure of (C) HPTP-B (red) (PDB entry 1XWW) and (D) DUSP14 (light green) (PDB entry 2WGP). The sulfate ion bound to the active site pocket of LmACR2 and the phosphate ion bound to DUSP14 are shown as ball-and-stick models with the oxygen, phosphorus, and sulfur atoms colored red, orange, and yellow, respectively. Cdc25A-cd, Cdc25B-cd, HPTP-B, and DUSP14 were superimposed on LmACR2 using COOT (*43*), and the figures were rendered using PYMOL (http://www.pymol.org).

The third family of arsenate reductases is also related to protein tyrosine phosphatases, although to a family of phosphatases different from that of pI258 ArsC. Several members of the family have been characterized to date: ScAcr2p from the yeast *Saccharomyces cerevisiae* (*11*, *12*), LmACR2 from the parasitic protozoan *Leishmania major* (*13*), PvACR2 from the fern *Pteris vittata* (*14*), OsACR2 from rice *Oryza sativa* (*15*), and AtACR2 from *Arabidopsis thaliana* (*16*, *17*). Like R773 ArsC, each of these eukaryotic arsenate reductases has a single active site cysteine residue and uses glutaredoxin and glutathione as reductants (*13*−*15*, *18*). Each of these proteins shows similarities in sequence in their active site region to the Cdc25 PTPase class of protein. However, these reductases also exhibit significant variability in their biochemical activities. Both ScAcr2p and PvACR2 lack phosphatase activity (*14*), although ScAcr2p can be converted from a reductase to a phosphatase by a small number of mutations (*19*). On the other hand, LmACR2, AtACR2, and OsACR2 exhibit both arsenate reductase and PTPase activities (*15*, *16*, *20*).

To date, no mammalian member of any of the three families of arsenate reductases has been identified, even though mammalian liver efficiently reduces As(V) to As(III) (*21*). It should be pointed out, however, that the relatedness of Acr2 enzymes to other members of the widespread protein tyrosine phosphatase family makes it difficult to identify homologues with arsenate reductase activity through a genomics approach. Three isoforms of Cdc25 have been identified in humans, Cdc25A, Cdc25B, and Cdc25C, each having several splice variants (*22*), and belong to the rhodanese/Cdc25 superfamily (*23*). These isoforms uniquely function to dephosphorylate phosphotyrosine and phosphothreonine residues on specific cyclin-dependent kinases, thus playing critical roles in G_1−S and G_2−M transitions, and in mitosis, thereby regulating cell division. The N-termini of Cdc25 enzymes are 20−25% identical in sequence with each other and contain several phosphorylation sites, as well as nuclear import and export signals (*24*). The C-termini of the Cdc25 PTPases are more than 60% similar in sequence with each other and contain the catalytic center.

The crystal structure of LmACR2 has been reported recently (*25*), as has the structure of a yeast homologue (*26*). Structural comparison between LmACR2 and the catalytic domains of human Cdc25 PTPases shows an overall structural similarity (Figure 1A,B). A DALI structural similarity comparison (*27*) of LmACR2 [Protein Data Bank (PDB) entry 2J6P] with the catalytic domains of human Cdc25A (PDB entry 1C25) (*28*) and Cdc25B (PDB entry 1QB0) (*29*) gives *Z* scores of 11.6 and 11.9, respectively. The active site loop conformation of LmACR2 is similar to that of the catalytic domain of the Cdc25 enzymes, and each contains a C-X_5-R signature motif, where C is the catalytic cysteine, the five X residues form a loop, and R is a highly conserved arginine. Structural comparison between LmACR2 and the catalytic domains of Cdc25A and

Cdc25B shows that the main chain root-mean-square deviations (rmsd) between equivalent active site loop C^{α} atoms are 0.54 and 0.18 Å, respectively (Figure 1B, inset). Whether the human Cdc25 enzymes have arsenate reductase activity cannot be deduced from their similarities with Acr2 enzymes. The objective of this study was to examine whether one of the human Cdc25 enzymes or more have an adventitious role as an arsenate reductase.

MATERIALS AND METHODS

Cloning of Human CDC25 Genes. The catalytic domains of human Cdc25A [residues 336−508 (GenBank accession number NP_001780)], Cdc25B [residues 377−550 (GenBank accession number NP_004349)], and Cdc25C [residues 280−454 (GenBank accession number NP_001781)] were cloned individually into a prokaryotic expression vector, thereby incorporating a start methionine and an N-terminal six-histidine tag. These proteins will henceforth be termed Cdc25A-cd (catalytic domain), Cdc25B-cd, and Cdc25C-cd, respectively. The catalytic domains of human Cdc25A, -B, and -C in the pET-3d vector (*24*) were kindly provided by J. Rudolph (Duke University School of Medicine, Durham, NC). A six-histidine tag was introduced into each of the *CDC25* constructs by PCR using *PfuTurbo* DNA polymerase (Stratagene). *CDC25A-cd* cDNA was amplified by PCR using the oligonucleotide primer pairs 5′-CGCTAGCGACCTTATAGGAGACTTCTC-3′ and 5′-GAAGCTTACCAGGTCCGGCTCTTGGT-3′. Similarly, *CDC25B-cd* cDNA was PCR amplified using the oligonucleotide primer pairs 5′-GCTAGCGAGCTGATTGGAGATTACTCT-3′ and 5′-GAAGCTTACCAGCTGCGAGTCTTGAG-3′. *CDC25C-cd* cDNA was amplified by PCR using the oligonucleotide primer pairs 5′-GCTAGCGGGCACCTGATTGGTGAT-3′ and 5′-GAAGCTTACTGCACTTTGCTCTGGCT-3′. Each PCR product was first cloned into the pGEM-T-Easy vector (Promega) and sequenced to confirm the integrity of the gene. Each of the constructs were next digested with NheI and HindIII, purified, and ligated to the NheI−HindIII sites of expression vector pET-28a (Novagen) in frame with the N-terminal six-histidine tag.

Full-length human *CDC25B* (GenBank accession number BC009953) in the pOTB7 vector was purchased from ATCC. *CDC25B* was amplified by PCR to introduce an NdeI site at the 5′-end and an XhoI site at the 3′-end using the forward and reverse primers 5′-CATATGGAGGTGCCCCAGCCG-3′ and 5′-CTCGAGTCACTGGTCCTGCAGCC-3′, respectively. The PCR product was first cloned into the pGEM-T-Easy vector, digested with NdeI and XhoI, and ligated to the NdeI−XhoI sites of expression vector pET-28a (Novagen) in frame with the N-terminal six-histidine tag.

Cloning of Human Glutaredoxin and Glutathione Reductase. Human glutaredoxin (*GLRX*) (GenBank accession number BC005304) in the pDNR-LIB vector was purchased from ATCC. The *GLRX* gene was amplified by PCR to introduce an NcoI site at the 5′-end and a NotI site at the 3′-end. The forward primer was 5′-CCATGGCTCAAGAGTTTGTGAACTGC-3′, and the reverse primer was 5′-GCGGCCGCCTGCAGAGCTCCAATCTG-3′. The amplified product was cloned into the pGEM-T-Easy vector. The resulting plasmid was digested with NcoI and NotI and inserted into the NcoI−NotI sites of pET-28b (Novagen) in frame with the C-terminal six-histidine tag.

Human glutathione reductase (GSR) was a gift from R. Heiner Schirmer (Heidelberg, Germany) and was provided as recombinant plasmid pUB302-2 (*30*). The *GSR* gene was amplified by PCR to introduce an NcoI site at the 5′-end and an XhoI site at the 3′-end. The forward and reverse primers were 5′-CAAACTGGAGACTGCCATGGCC-3′ and 5′-CTCGAGACGAAGTGTGACCAGCTC-3′, respectively. The amplified product was cloned into the pGEM-T-Easy vector. The resulting plasmid was digested with NcoI and XhoI and inserted into the NcoI−XhoI sites of pET-28b (Novagen) in frame with the C-terminal six-histidine tag.

Oligonucleotide-Directed Mutagenesis. Mutations in *CDC25B-cd* were introduced by site-directed mutagenesis using the QuikChange site-directed mutagenesis procedure (Stratagene). The mutagenic oligonucleotides used for both strands and the respective changes introduced (underlined) are as follows: C120A, 5′-CCTCATTTTCCACGCTGAATTCTCATCTG-3′ and 5′-CAGATGAGAATTCAGCGTGGAAAATGAGG-3′; R126A, 5′-CTCATCTGAGGCTGGGCCCCGCATG-3′ and 5′-CATGCGGGGCCCAGCCTCAGATGAG-3′. Each mutation was confirmed by sequencing the entire gene using the CEQ 2000 DNA Analysis System (Beckman Coulter).

Protein Purification. Cells of *E. coli* strain Rosetta 2 (DE3) (Novagen) bearing any of the *CDC25* genes (*CDC25A-cd*, *CDC25B-cd*, *CDC25B*, or *CDC25C-cd*) in vector plasmid pET-28a were grown in 4 L of Luria-Bertani medium (*31*) containing 50 μg/mL kanamycin and 34 μg/mL chloramphenicol with shaking at 37 °C. At an A_{600} of 0.5, the culture temperature was reduced to 16 °C, IPTG was added as an inducer to a final concentration of 0.1 mM, and the culture was grown for an additional 16 h at 16 °C. The cells were washed once with 10 mM Tris-HCl (pH 7.5) containing 0.1 M KCl. Cells were next suspended in buffer A [25 mM Bis-Tris propane (pH 8.0), 20 mM imidazole, 0.5 M NaCl, 10 mM β-mercaptoethanol, and 20% glycerol] at a ratio of 5 mL of buffer/g of wet cells and lysed by a single passage through a French pressure cell at 20000 psi. Diisopropyl fluorophosphate (2.5 μL/g of wet cells) was added to the lysate immediately after lysis. Membranes and unbroken cells were removed by centrifugation at 150000*g* for 1 h, and the supernatant was loaded at a flow rate of 0.5 mL/min onto a 10 mL Ni^{2+}-nitrilotriacetic acid column (Qiagen) preequilibrated with buffer A. The column was then washed with 300 mL of buffer A followed by elution with 125 mL of buffer A in which the concentration of imidazole was increased to 200 mM. Cdc25-containing fractions were identified by sodium dodecyl sulfate−polyacrylamide gel electrophoresis (SDS−PAGE), pooled, concentrated by centrifugation using a 10 kDa cutoff Amicon ultracentrifugal filter (Millipore), and stored in 25 mM Bis-Tris propane (pH 8.0), 0.2 M NaCl, 2 mM EDTA, 10 mM β-mercaptoethanol, and 20% glycerol at −80 °C.

For purification of GLRX and GSR, cells of *E. coli* strain Rosetta 2 (DE3) bearing either the *GLRX* or *GSR* gene in vector plasmid pET-28b were grown in 4 L of Luria-Bertani medium (*31*), containing 50 μg/mL kanamycin and 34 μg/mL chloramphenicol, with shaking at 37 °C. At an A_{600} of 0.5, IPTG was added as an inducer to a final concentration of 0.1 mM, and the culture was grown for an additional 3 h at 37 °C. Both proteins were purified as described above except that GLRX and GSR were concentrated by centrifugation using 5 and 30 kDa cutoff Amicon ultracentrifugal filters (Millipore), respectively. Protein concentrations were determined from the absorbance at 280 nm using the following extinction coefficients calculated with the ExPASy ProtParam tool (http://us.expasy.org/tools/protparam.html): 23630 M^{-1} cm^{-1} for Cdc25A-cd, 22140 M^{-1} cm^{-1} for Cdc25B-cd, 19870 M^{-1} cm^{-1} for Cdc25C-cd, 3230 M^{-1} cm^{-1} for GLRX, and 36370 M^{-1} cm^{-1} for GSR.

Assay of Phosphatase Activity. The phosphatase activities of human Cdc25-cd proteins were measured from the rate of hydrolysis of *p*-nitrophenyl phosphate (pNPP) (*32*). The assay mixture containing 0.25−0.75 μM Cdc25A-cd, -B-cd, or -C-cd in buffer B [50 mM Tris-HCl (pH 8.5), 50 mM NaCl, 1 mM EDTA, and 0.1 mg/mL BSA] was incubated at 30 °C for 5 min in a 96-well plate (180 μL/well). The reaction was initiated by the addition of increasing concentrations of pNPP (20 μL/well), yielding a final volume of 200 μL/well. pNPP hydrolysis was followed by monitoring the increase in absorbance at 405 nm (ε = 18.8 mM^{-1} cm^{-1}) using a SpectraMax 340PC microplate reader (Molecular Devices). The PathCheck feature of the microplate reader was used to automatically normalize absorbance values to a 1 cm path length. The data were analyzed using SigmaPlot version 11.0. Each assay was repeated at least three times with two separate batches of purified protein.

Assay of Arsenate Reductase Activity. Arsenate reductase activity was assayed at 30 °C using a coupled assay method (*18*) with the following modifications. The assay mixture in buffer B containing any one of the Cdc25-cd enzymes at ∼10 μM, 0.25 mM NADPH, 2 mM GSH, 85 nM GSR, and the indicated concentrations of sodium arsenate was incubated at 30 °C for 5 min in a 96-well plate (190 μL/well). The assay was initiated by the addition of 1.5 μM GLRX (10 μL/well), yielding a final volume of 200 μL/well. Arsenate reduction coupled to NADPH oxidation was monitored by following the decrease in absorbance at 340 nm ($\Delta\varepsilon_{340}$ = 6.2 mM^{-1} cm^{-1}) using a SpectraMax 340PC microplate reader. The PathCheck feature of the microplate reader was used to automatically normalize absorbance values to a 1 cm path length. The data were analyzed using SigmaPlot version 11.0. Each assay was repeated at least three times with two separate batches of purified protein.

Cdc25B-cd-catalyzed reduction of As(V) to As(III) was also monitored by HPLC (Series 2000, PerkinElmer) ICP-MS (ELAN 9000, PerkinElmer). Cdc25B-cd (10 μM) was incubated with 1 mM sodium arsenate at 30 °C for 5 min in buffer B containing 0.25 mM NADPH, 85 nM GSR, and 2 mM GSH. The reaction was initiated with 1.5 μM GLRX, and the decrease in NADPH absorbance at 340 nm was followed until there was no further decrease. The reaction mixture was passed through a 3 kDa cutoff Microcon centrifugal filter (Millipore) and the filtrate diluted 500-fold with HPLC grade water. Arsenic speciation of the diluted filtrate was conducted using a Jupiter 300 C18 reverse phase column (Phenomenex) and eluted isocratically with a mobile phase consisting of 3 mM malonic acid, 5 mM tetrabutylammonium hydroxide, and 5% methanol (pH 5.6), with a flow rate of 1 mL/min (*33*).

Inhibitor Studies. Cdc25B-cd (0.25 μM) was preincubated with increasing concentrations of sodium arsenite [As(III)], sodium arsenate [As(V)], monomethylarsonic acid [MAs(V)], or dimethylarsinic acid [DMAs(V)] in buffer B at 30 °C. The reaction was initiated with different fixed concentrations of pNPP. The graphs were plotted, and the best fit of the data was calculated using SigmaPlot version 11.0.

RESULTS

Phosphatase Activity of Cdc25A-cd, Cdc25B-cd, and Cdc25C-cd. The catalytic domains of Cdc25A, -B, and -C were PCR amplified and cloned behind the T7 promoter of prokaryotic expression vector pET-28a. This introduced a vector-derived 23-amino acid extension at the N-terminus of each construct which includes a start methionine and a six-histidine tag. Upon overexpression in *E. coli*, each Cdc25 derivative was found to be soluble in the cytosol and was purified to >90% homogeneity by nickel affinity chromatography. The phosphatase activities of each of these proteins were determined using the artificial substrate pNPP. The reaction showed a broad pH optimum between pH 8 and 9, which declined sharply above and below these pH values (Figure S1 of the Supporting Information). All kinetic experiments were therefore conducted at pH 8.5. Table 1 shows that the K_m values of each of these proteins are in the millimolar range. These values are in reasonable agreement with those measured previously for either the GST-fused or untagged Cdc25-cd constructs (*24*, *34*−*36*). The k_{cat} and k_{cat}/K_m values of pNPP for Cdc25B-cd were 0.3 s^{-1} and 33 M^{-1} s^{-1}, respectively, at pH 8.5 and 30 °C. Under these experimental conditions, Cdc25B-cd exhibited 5- and 7-fold enhancements of catalytic efficiency over Cdc25A-cd and Cdc25C-cd, respectively (Table 1). Further experiments were therefore conducted with Cdc25B-cd.

Table 1: Kinetic Parameters of the Phosphatase Activity of Cdc25-cd Enzymes

protein	pNPP K_m (mM)	k_{cat} (s^{-1})	k_{cat}/K_m (M^{-1} s^{-1})
$[His]_6$-Cdc25A-cd	25 ± 1.6	0.18 ± 0.004	7 ± 0.5
$[His]_6$-Cdc25B-cd	9 ± 1	0.3 ± 0.006	33 ± 3
$[His]_6$-Cdc25C-cd	26 ± 1.4	0.12 ± 0.003	4.6 ± 0.2

Competitive Inhibition of Cdc25B-cd Phosphatase Activity. As(III), As(V), MAs(V), and DMAs(V) were tested for their ability to inhibit Cdc25B-cd-catalyzed phosphatase activity. Dixon plots of $1/v$ versus the inhibitor As(V) in the presence of various fixed concentrations of the substrate pNPP are shown in Figure 2. A replot of the slopes of the Dixon plots versus the reciprocal of pNPP concentration shows a straight line passing through the origin (Figure 2, inset), which indicates that As(V) is a competitive inhibitor of Cdc25B-cd phosphatase activity, with an apparent K_i of 0.4 mM. In contrast, As(III) exhibited a 10-fold lower affinity than As(V), with an apparent K_i of 4 mM (Figure S2 of the Supporting Information). MAs(V) was a slightly better inhibitor than As(III), with an apparent K_i of 2 mM (Figure S3 of the Supporting Information). DMAs(V) did not inhibit Cdc25B-cd phosphatase activity (data not shown).

Arsenate Reductase Activity of Cdc25B-cd and Cdc25C-cd. Since As(V) competes with the phosphatase substrate pNPP for the same binding site, the ability of Cdc25B-cd to reduce arsenate was examined. The coupled assay used for measuring ScAcr2p activity was adapted for measuring Cdc25B-cd activity. In this reaction scheme, GSH serves as the electron donor for As(V) reduction, forming a mixed disulfide with the enzyme. Through thiol exchange with yeast glutaredoxin (Grx1p), the enzyme sulfhydryl is regenerated with the formation of glutathionylated glutaredoxin (Grx-SG), which is finally reduced by GSH, and the oxidized glutathione (GSSG) is reduced by yeast glutathione reductase with NADPH as the ultimate source of reducing potential (*18*). In the presence of purified Cdc25B-cd, Grx1p, and arsenate, oxidation of NADPH was observed, reflecting reduction of arsenate to arsenite (Figure 3). Reductase activity required the presence of each component in the assay medium. In the absence of any, there was only a basal rate of NADPH oxidation (Figure 3). The K_m of Cdc25B-cd for As(V) was 1.8 mM, and the k_{cat} was 0.010 s^{-1}, at pH 8.5 and 30 °C (Figure S4 of the Supporting Information).

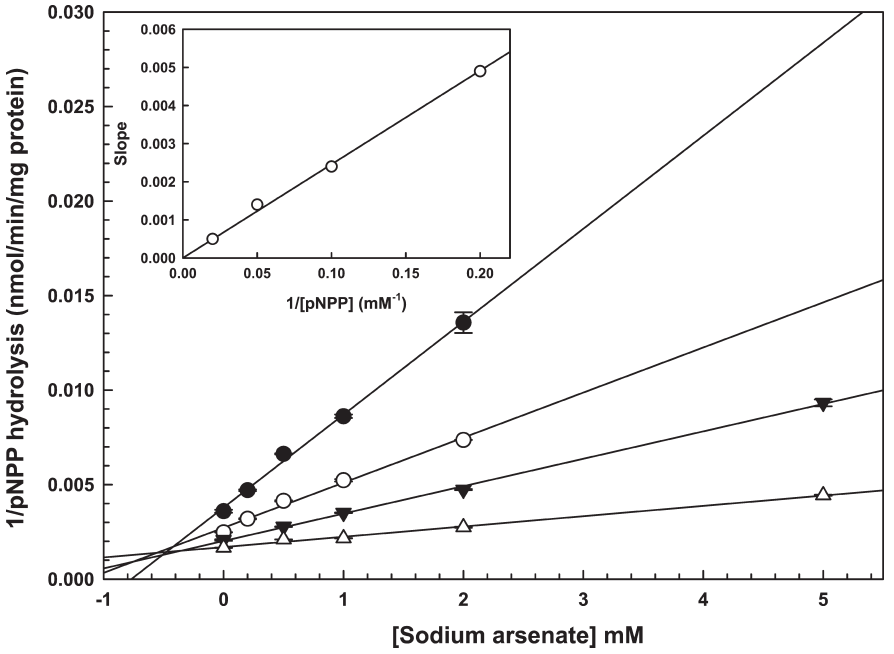

FIGURE 2: Inhibition of Cdc25B-cd-catalyzed phosphatase activity. The Dixon plots show the dephosphorylation rates of 5 (●), 10 (○), 20 (▼) and 50 mM pNPP (△) when assayed in the presence of the indicated concentrations of the inhibitor As(V). The error bars represent the standard errors from two independent assays. The inset shows a replot of the slopes of the Dixon plots; K_i was estimated using the equation $K_i = K_m/(V_{max} \times$ slope).

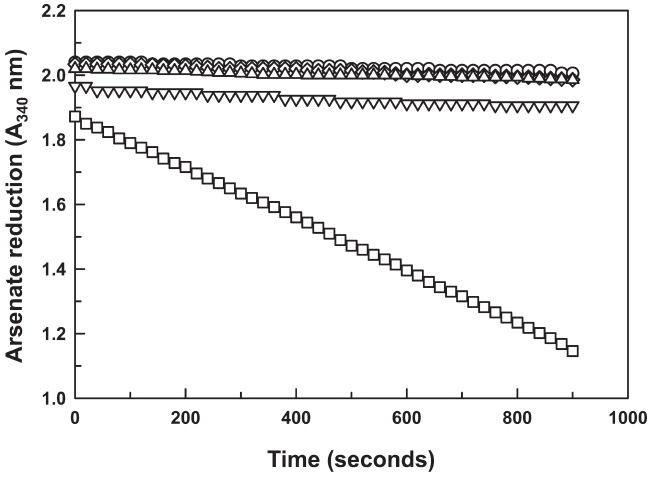

FIGURE 3: Requirements for Cdc25B-cd arsenate reductase. Arsenate reductase activity was estimated from the oxidation of NADPH measured at 340 nm, as described in Materials and Methods: (○) 15 μM Cdc25B-cd, 50 mM sodium arsenate, and 2 mM GSH, (▽) 1 μM Grx1p, 50 mM sodium arsenate, and 2 mM GSH, (□) 15 μM Cdc25B-cd, 1 μM Grx1p, 50 mM sodium arsenate, and 2 mM GSH, (△) 15 μM Cdc25B-cd, 1 μM Grx1p, and 2 mM GSH, and (◇) 15 μM Cdc25B-cd, 1 μM Grx1p, and 50 mM sodium arsenate.

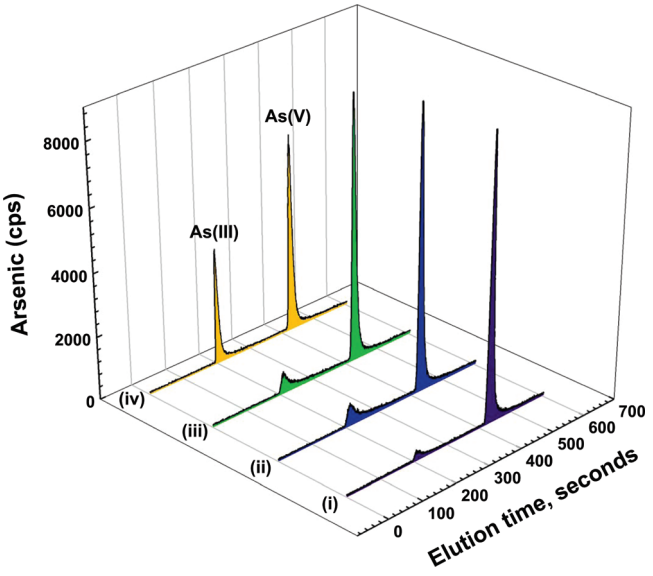

FIGURE 4: Purified Cdc25B-cd catalyzes the reduction of arsenate. Arsenic speciation of the reaction solution was performed by reverse phase HPLC coupled to ICP-MS, with the relative amounts of arsenic expressed as counts per second. The reactions were performed in buffer B containing 85 nM GSR and as described in Materials and Methods: (i) 1 mM sodium arsenate only, (ii) 1 mM sodium arsenate, 0.25 mM NADPH, 2 mM GSH, and 10 μM Cdc25B-cd, (iii) 1 mM sodium arsenate, 0.25 mM NADPH, 2 mM GSH, and 1.5 μM GLRX, and (iv) 1 mM sodium arsenate, 0.25 mM NADPH, 2 mM GSH, 1.5 μM GLRX, and 10 μM Cdc25B-cd.

Since the Cdc25s are human proteins, the ability of human glutaredoxin (GLRX) and human glutathione reductase (GSR) to serve as cofactors in Cdc25B-cd catalyzed As(V) reduction was examined. The genes for GLRX and GSR were cloned and expressed in *E. coli*, and the protein products were purified. The ability of Cdc25B-cd to reduce As(V) was examined by ion exchange HPLC separation of trivalent and pentavalent arsenicals and the amount of each species quantified by ICP-MS. In the presence of glutathione, GLRX, and GSR, Cdc25B-cd was found to catalyze the reduction of As(V) to As(III) (Figure 4). There was no As(V) reduction when any one of the components was omitted (Figure 4).

The kinetic parameters of Cdc25B-cd catalyzed As(V) reduction in the presence of GSH and GLRX were examined in greater detail using the coupled spectrophotometric assay method described earlier. Cdc25B-cd-catalyzed As(V) reduction showed a pH optimum of 8.5 at 30 °C (Figure S5 of the Supporting Information). As(V) reduction by Cdc25B-cd followed hyperbolic kinetics (Figure 5). The K_m and k_{cat} for the reaction are

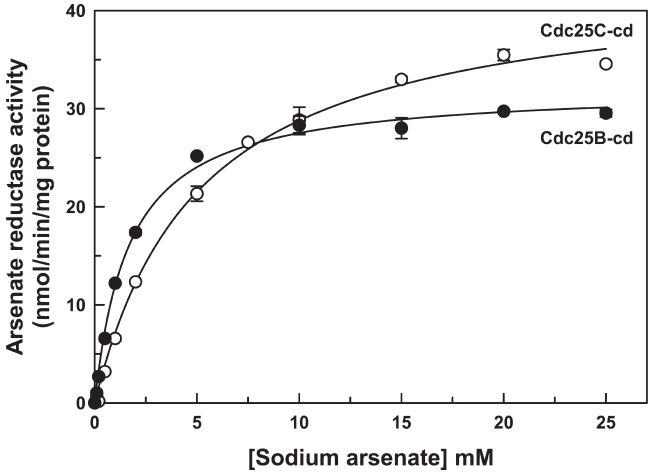

FIGURE 5: Arsenate reductase activity of purified Cdc25B-cd and Cdc25C-cd. The arsenate reductase activities of Cdc25B-cd (●) and Cdc25C-cd (○) were assayed with 2 mM GSH, 1.5 μM GLRX, and 85 nM GSR. The rate of arsenate reductase activity was estimated from the oxidation of NADPH measured at 340 nm at each concentration of sodium arsenate, as described in Materials and Methods. The error bars represent standard deviations (n = 3).

Table 2: Kinetic Parameters of the Arsenate Reductase Activity of Cdc25-cd Enzymes with 2 mM GSH

protein	K_m (mM)	k_{cat} (s^{-1})	k_{cat}/K_m (M^{-1} s^{-1})
$[His]_6$-Cdc25B-cd	1.7 ± 0.1	0.012	7 ± 0.5
$[His]_6$-Cdc25C-cd	5 ± 0.3	0.017	3.4 ± 0.2

described in Table 2. Similarly, Cdc25C-cd also catalyzed As(V) reduction utilizing GSH and GLRX as sources of reducing potential (Figure 5 and Table 2). However, whether Cdc25A-cd can catalyze As(V) reduction could not be determined, as addition of Cdc25A-cd led to precipitation in the assay medium. Neither Cdc25B-cd nor CDC25C-cd could reduce MAs(V) under the conditions of the assay (data not shown). The studies described above were conducted in the presence of 2 mM GSH. Interestingly, when the GSH concentration in the assay protocol was increased to 5 mM, a concentration present in many mammalian cells, the affinity of either Cdc25B-cd or Cdc25C-cd for As(V) increased by 2-fold and the turnover number increased similarly (cf. Tables 2 and 3). Thus, the Cdc25 enzymes become even better arsenate reductases in the presence of an increased concentration of GSH.

The rate of As(V) reduction as a function of human GLRX concentration at a saturating concentration of sodium arsenate was also determined (Figure 6). The activity was hyperbolic as a function of GLRX concentration (Figure 6). The K_m values of Cdc25B-cd and Cdc25C-cd for GLRX were calculated to be 95 and 175 nM, respectively. The results demonstrate that human glutaredoxin is as effective as the yeast homologue in supporting Cdc25-cd-catalyzed As(V) reduction.

Effect of Alteration of the Active Site Residues of Cdc25B-cd. As discussed earlier, the active site of each of the Cdc25-cds contains a C-X_5-R signature motif (Figure 1). Mutation of the cysteine or arginine residues in the active site motif resulted in the complete loss of Cdc25 phosphatase activity (*34*). To determine whether the Cdc25 catalytic domain shares the same active site for arsenate reduction, the conserved cysteine or arginine residues were modified individually to alanines by site-directed

Table 3: Kinetic Parameters of the Arsenate Reductase Activity of Cdc25-cd Enzymes with 5 mM GSH

protein	K_m (mM)	k_{cat} (s^{-1})	k_{cat}/K_m (M^{-1} s^{-1})
$[His]_6$-Cdc25B-cd	0.9 ± 0.04	0.025	28 ± 1
$[His]_6$-Cdc25C-cd	2.5 ± 0.1	0.03	12 ± 0.5

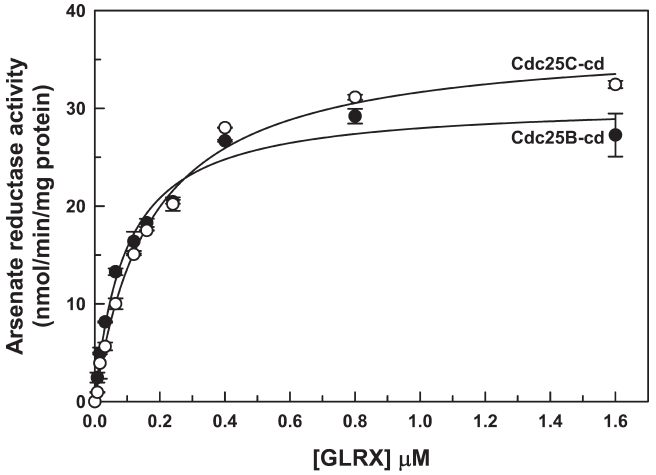

FIGURE 6: Human glutaredoxin (GLRX) as an electron donor for Cdc25B-cd- and Cdc25C-cd-catalyzed As(V) reduction. The arsenate reductase activities of Cdc25B-cd (●) and Cdc25C-cd (○) were assayed with 2 mM GSH, 15 mM sodium arsenate, and 85 nM GSR. The rate of arsenate reductase activity was estimated from the oxidation of NADPH measured at 340 nm at each concentration of GLRX, as described in Materials and Methods. The error bars represent standard deviations (n = 3).

mutagenesis, generating C120A and R126A Cdc25B-cd. Each altered protein was purified by nickel affinity chromatography. Both C120A and R126A Cdc25B-cd preparations were completely inactive when analyzed for either phosphatase or arsenate reductase activity (data not shown), even at 5−7-fold higher concentrations of enzyme. These results suggest that the Cdc25 catalytic domain shares the same active site for dephosphorylation and arsenate reduction.

DISCUSSION

Since the active site of human Cdc25 phosphatases shows great structural similarity to the *Leishmania* arsenate reductase LmACR2 (Figure 1), our objective was to determine whether the human Cdc25 enzymes also adventitiously catalyze arsenate reduction. The results clearly demonstrate that both Cdc25B-cd and Cdc25C-cd exhibit arsenate reductase activity. However, the rate of arsenate reduction was 25-and 7-fold lower than the rates of dephosphorylation reaction for Cdc25B-cd and Cdc25C-cd, respectively (cf. Tables 1 and 2). Although either As(V) or MAs(V) competitively inhibited Cdc25B-cd phosphatase activity (Figure 2), the enzyme reduced only As(V) but not MAs(V). In comparison with known arsenate reductases, the Cdc25-cd enzymes (Table 2) exhibit an ~5-fold higher rate of turnover than LmACR2 (*13*), but an ~20-fold lower rate of turnover than *E. coli* plasmid R773 ArsC (*5*). However, it should be noted that the assay conditions are not identical. While LmACR2 and R773 ArsC were assayed at their optimal pH of 6.5 in the presence of 1 mM GSH, Cdc25-cd-catalyzed arsenate reduction was monitored at pH 8.5 in the presence of 2 mM GSH (Table 2). The Cdc25 enzymes showed even higher arsenate reductase activity

when the GSH concentration was increased to 5 mM (Table 3). Whether a similar increase in GSH concentration will improve the catalytic turnover of R773 ArsC or Acr2 enzymes has not been reported in the literature.

Arsenate reduction by both Cdc25s and Acr2 reductases likely utilizes the cysteine and arginine residues of the C-X_5-R active site loop, as their substitution by mutagenesis leads to a loss of activity in both. Although both Cdc25B-cd and Cdc25C-cd contain the CEFSSER phosphate binding loop, their phosphatase and reductase activities are not identical, suggesting that other residues affect the activities of each of the enzymes differently.

The data also demonstrate that both human Cdc25B-cd and Cdc25C-cd reduce As(V) in the presence of GLRX and GSR, suggesting that this may be the coupled system for the reduction of As(V) in human cells. It should be noted that most of the studies with human Cdc25 enzymes, including purification, characterization, and crystallization, have been performed with the catalytic domain and not the full-length enzyme (*28*, *29*, *34*, *35*, *37*). Whether the full-length Cdc25 phosphatase can reduce As(V) was examined. When full-length Cdc25B with an N-terminal six-histidine tag was expressed in *E. coli*, all of the protein was found in inclusion bodies, precluding biochemical characterization.

Cdc25 phosphatase belongs to the PTPase superfamily that, in addition to Cdc25, consists of three other subfamilies: classical PTPases, dual specific PTPases, and low-molecular weight PTPases (*38*). Apart from the seven-amino acid C-X_5-R loop at the active site, these four subfamilies share little sequence similarity. The human genome is estimated to contain more than 100 PTPases, each containing the same conserved structural feature at their active site and each employing a similar catalytic mechanism (*38*). The structure of the active site pockets of HPTP-B (PDB entry 1XWW) (*39*), a human isoenzyme of the LMW PTPase category, and human dual-specificity phosphatase 14, DUSP14 (PDB entry 2WGP) (*40*), are very similar to that of LmACR2. Structural comparison between LmACR2 and either HPTP-B or DUSP14 shows that the rmsd for the overall structure is 2.46 or 2.65 Å, respectively, while the rmsd between equivalent C^{α} atoms of the active site loop is 0.27 or 0.33 Å, respectively (Figure 1). It should be noted that the active site of the bacterial pI258 ArsC is similar to that of LmACR2, even though they are apparently unrelated. The rmsd between equivalent C^{α} atoms of the active site loop is 0.54 Å (*25*), and pI258 ArsC shows both arsenate reductase and phosphatase activities (*2*).

In summary, the experiments described in this paper clearly demonstrate that human Cdc25 enzymes are capable of catalyzing As(V) reduction. Since Cdc25 phosphatase activity is high in dividing cells and its overexpression has been reported in a variety of human cancer tissues (*41*), it is likely that arsenate reductase activity will be higher in such cell types, leading to increased arsenic toxicity. Considering that many other PTPases are expressed in various human cells and tissues, this study also provides an approach to determining whether other PTPase family members have similar adventitious activity. Chronic arsenic poisoning caused by arsenic contamination of drinking water has affected millions of people in many regions of the world (*42*), and these results contribute to our understanding of the pathways for human arsenic metabolism.

SUPPORTING INFORMATION AVAILABLE

Additional experimental results. This material is available free of charge via the Internet at http://pubs.acs.org.

REFERENCES

1. Abernathy, C. O., Thomas, D. J., and Calderon, R. L. (2003) Health effects and risk assessment of arsenic. *J. Nutr. 133*, 1536S–1538S.
2. Messens, J., and Silver, S. (2006) Arsenate reduction: Thiol cascade chemistry with convergent evolution. *J. Mol. Biol. 362*, 1–17.
3. Bhattacharjee, H., and Rosen, B. P. (2007) Arsenic Metabolism in Prokaryotic and Eukaryotic Microbes. In Molecular Microbiology of Heavy Metals (Nies, D. H., and Silver, S., Eds.) pp 371−406, Springer, Berlin.
4. Gregus, Z., Roos, G., Geerlings, P., and Nemeti, B. (2009) Mechanism of thiol-supported arsenate reduction mediated by phosphorolytic-arsenolytic enzymes: II. Enzymatic formation of arsenylated products susceptible for reduction to arsenite by thiols. *Toxicol. Sci. 110*, 282–292.
5. Shi, J., Vlamis-Gardikas, A., Åslund, F., Holmgren, A., and Rosen, B. P. (1999) Reactivity of glutaredoxins 1, 2, and 3 from *Escherichia coli* shows that glutaredoxin 2 is the primary hydrogen donor to ArsC-catalyzed arsenate reduction. *J. Biol. Chem. 274*, 36039–36042.
6. Ji, G., and Silver, S. (1992) Reduction of arsenate to arsenite by the ArsC protein of the arsenic resistance operon of *Staphylococcus aureus* plasmid pI258. *Proc. Natl. Acad. Sci. U.S.A. 89*, 9474–9478.
7. Ji, G., Garber, E. A. E., Armes, L. G., Chen, C. M., Fuchs, J. A., and Silver, S. (1994) Arsenate reductase of *Staphylococcus aureus* plasmid pI258. *Biochemistry 33*, 7294–7299.
8. Messens, J., Hayburn, G., Desmyter, A., Laus, G., and Wyns, L. (1999) The essential catalytic redox couple in arsenate reductase from *Staphylococcus aureus*. *Biochemistry 38*, 16857–16865.
9. Zegers, I., Martins, J. C., Willem, R., Wyns, L., and Messens, J. (2001) Arsenate reductase from *S. aureus* plasmid pI258 is a phosphatase drafted for redox duty. *Nat. Struct. Biol. 8*, 843–847.
10. Meng, Y. L., Liu, Z., and Rosen, B. P. (2004) As(III) and Sb(III) uptake by GlpF and efflux by ArsB in *Escherichia coli*. *J. Biol. Chem. 279*, 18334–18341.
11. Bobrowicz, P., Wysocki, R., Owsianik, G., Goffeau, A., and Ulaszewski, S. (1997) Isolation of three contiguous genes, *ACR1*, *ACR2* and *ACR3*, involved in resistance to arsenic compounds in the yeast *Saccharomyces cerevisiae*. *Yeast 13*, 819–828.
12. Mukhopadhyay, R., and Rosen, B. P. (1998) *Saccharomyces cerevisiae ACR2* gene encodes an arsenate reductase. *FEMS Microbiol. Lett. 168*, 127–136.
13. Zhou, Y., Messier, N., Ouellette, M., Rosen, B. P., and Mukhopadhyay, R. (2004) *Leishmania major* LmACR2 is a pentavalent antimony reductase that confers sensitivity to the drug pentostam. *J. Biol. Chem. 279*, 37445–37451.
14. Ellis, D. R., Gumaelius, L., Indriolo, E., Pickering, I. J., Banks, J. A., and Salt, D. E. (2006) A novel arsenate reductase from the arsenic hyperaccumulating fern *Pteris vittata*. *Plant Physiol. 141*, 1544–1554.
15. Duan, G. L., Zhou, Y., Tong, Y. P., Mukhopadhyay, R., Rosen, B. P., and Zhu, Y. G. (2007) A CDC25 homologue from rice functions as an arsenate reductase. *New Phytol. 174*, 311–321.
16. Bleeker, P. M., Hakvoort, H. W., Bliek, M., Souer, E., and Schat, H. (2006) Enhanced arsenate reduction by a CDC25-like tyrosine phosphatase explains increased phytochelatin accumulation in arsenate-tolerant *Holcus lanatus*. *Plant J. 45*, 917–929.
17. Dhankher, O. P., Rosen, B. P., McKinney, E. C., and Meagher, R. B. (2006) Hyperaccumulation of arsenic in the shoots of *Arabidopsis* silenced for arsenate reductase (ACR2). *Proc. Natl. Acad. Sci. U.S.A. 103*, 5413–5418.
18. Mukhopadhyay, R., Shi, J., and Rosen, B. P. (2000) Purification and characterization of Acr2p, the *Saccharomyces cerevisiae* arsenate reductase. *J. Biol. Chem. 275*, 21149–21157.
19. Mukhopadhyay, R., Zhou, Y., and Rosen, B. P. (2003) Directed evolution of a yeast arsenate reductase into a protein-tyrosine phosphatase. *J. Biol. Chem. 278*, 24476–24480.
20. Zhou, Y., Bhattacharjee, H., and Mukhopadhyay, R. (2006) Bifunctional role of the leishmanial antimonate reductase LmACR2 as a protein tyrosine phosphatase. *Mol. Biochem. Parasitol. 148*, 161–168.
21. Radabaugh, T. R., and Aposhian, H. V. (2000) Enzymatic reduction of arsenic compounds in mammalian systems: Reduction of arsenate to arsenite by human liver arsenate reductase. *Chem. Res. Toxicol. 13*, 26–30.
22. Kristjansdottir, K., and Rudolph, J. (2004) Cdc25 phosphatases and cancer. *Chem. Biol. 11*, 1043–1051.
23. Bordo, D., and Bork, P. (2002) The rhodanese/Cdc25 phosphatase superfamily. Sequence-structure-function relations. *EMBO Rep. 3*, 741–746.
24. Rudolph, J., Epstein, D. M., Parker, L., and Eckstein, J. (2001) Specificity of natural and artificial substrates for human Cdc25A. *Anal. Biochem. 289*, 43–51.

25. Mukhopadhyay, R., Bisacchi, D., Zhou, Y., Armirotti, A., and Bordo, D. (2009) Structural characterization of the As/Sb reductase LmACR2 from *Leishmania major*. *J. Mol. Biol. 386*, 1229–1239.
26. Yeo, H. K., and Lee, J. Y. (2009) Crystal structure of *Saccharomyces cerevisiae* Ygr203w, a homolog of single-domain rhodanese and Cdc25 phosphatase catalytic domain. *Proteins 76*, 520–524.
27. Holm, L., and Sander, C. (1995) Dali: A network tool for protein structure comparison. *Trends Biochem. Sci. 20*, 478–480.
28. Fauman, E. B., Cogswell, J. P., Lovejoy, B., Rocque, W. J., Holmes, W., Montana, V. G., Piwnica-Worms, H., Rink, M. J., and Saper, M. A. (1998) Crystal structure of the catalytic domain of the human cell cycle control phosphatase, Cdc25A. *Cell 93*, 617–625.
29. Reynolds, R. A., Yem, A. W., Wolfe, C. L., Deibel, M. R., Jr., Chidester, C. G., and Watenpaugh, K. D. (1999) Crystal structure of the catalytic subunit of Cdc25B required for G2/M phase transition of the cell cycle. *J. Mol. Biol. 293*, 559–568.
30. Nordhoff, A., Bucheler, U. S., Werner, D., and Schirmer, R. H. (1993) Folding of the four domains and dimerization are impaired by the Gly446 → Glu exchange in human glutathione reductase. Implications for the design of antiparasitic drugs. *Biochemistry 32*, 4060–4066.
31. Sambrook, J., and Russell, D. (2001) Molecular Cloning: A Laboratory Manual, 3rd ed., Cold Spring Harbor Laboratory Press, Plainview, NY.
32. Montalibet, J., Skorey, K. I., and Kennedy, B. P. (2005) Protein tyrosine phosphatase: Enzymatic assays. *Methods 35*, 2–8.
33. Qin, J., Rosen, B. P., Zhang, Y., Wang, G., Franke, S., and Rensing, C. (2006) Arsenic detoxification and evolution of trimethylarsine gas by a microbial arsenite S-adenosylmethionine methyltransferase. *Proc. Natl. Acad. Sci. U.S.A. 103*, 2075–2080.
34. Xu, X., and Burke, S. P. (1996) Roles of active site residues and the NH_2-terminal domain in the catalysis and substrate binding of human Cdc25. *J. Biol. Chem. 271*, 5118–5124.
35. Gottlin, E. B., Xu, X., Epstein, D. M., Burke, S. P., Eckstein, J. W., Ballou, D. P., and Dixon, J. E. (1996) Kinetic analysis of the catalytic domain of human Cdc25B. *J. Biol. Chem. 271*, 27445–27449.
36. Chen, W., Wilborn, M., and Rudolph, J. (2000) Dual-specific Cdc25B phosphatase: In search of the catalytic acid. *Biochemistry 39*, 10781–10789.
37. Eckstein, J. W., Beer-Romero, P., and Berdo, I. (1996) Identification of an essential acidic residue in Cdc25 protein phosphatase and a general three-dimensional model for a core region in protein phosphatases. *Protein Sci. 5*, 5–12.
38. Zhang, Z. Y. (2003) Chemical and mechanistic approaches to the study of protein tyrosine phosphatases. *Acc. Chem. Res. 36*, 385–392.
39. Zabell, A. P., Schroff, A. D., Jr., Bain, B. E., Van Etten, R. L., Wiest, O., and Stauffacher, C. V. (2006) Crystal structure of the human B-form low molecular weight phosphotyrosyl phosphatase at 1.6-Å resolution. *J. Biol. Chem. 281*, 6520–6527.
40. Lountos, G. T., Tropea, J. E., Cherry, S., and Waugh, D. S. (2009) Overproduction, purification and structure determination of human dual-specificity phosphatase 14. *Acta Crystallogr. D65*, 1013–1020.
41. Kiyokawa, H., and Ray, D. (2008) In vivo roles of CDC25 phosphatases: Biological insight into the anti-cancer therapeutic targets. *Anticancer Agents Med. Chem. 8*, 832–836.
42. Subcommittee to Update the 1999 Arsenic in Drinking Water Report, N. R. C. (2001) Arsenic in Drinking Water: 2001 Update, The National Academies Press, Washington, DC.
43. Emsley, P., and Cowtan, K. (2004) Coot: Model-building tools for molecular graphics. *Acta Crystallogr. D60*, 2126–2132.